

Encoding Morphology in Oxide Nanostructures during Their Growth

Yigal Lilach,^{*,†} Jin-Ping Zhang,[‡] Martin Moskovits,[†] and Andrei Kolmakov[§]

Department of Chemistry & Biochemistry and Department of Materials, University of California, Santa Barbara, California 93106, and Physics Department, SIUC, Carbondale, Illinois 62901

Received August 5, 2005; Revised Manuscript Received September 4, 2005

ABSTRACT

Programmable control over the overall structure of SnO₂ nanowires grown by vapor-solid synthesis is shown to be possible by pulse modulating the flow rate of the carrier gas in which oxygen (one of the reactants) is entrained. The control is shown to depend on the local oscillation of the supersaturation condition for the SnO vapor (another reactant) in the vicinity of the growing nanostructure. The latter triggers dramatic, reproducible oscillations in the lateral dimensions of the nanostructure and in the direction of its growth. The method provides a means for producing predictable morphological and compositional variations in 1D nanostructures, thereby potentially resulting in a high yield of custom-designed nanostructures.

The great recent interest in one-dimensional (1D) semiconducting nanostructures is based on their proposed and preliminarily demonstrated operation as ultrasmall active elements in applications such as nanoelectronics, optoelectronics, lasers, chemical and biological sensors, and energy conversion devices.^{1,2} Among the materials from which nanostructures have been fashioned, SnO₂ has received a great deal of recent attention^{3–9} primarily because of its promise in sensors and other electronic and optoelectronic¹⁰ devices and also because of its ability to form a multitude of unusual nanostructures including belts, disks, and zig-zags.¹¹ To conform with the requirements of these varied functions, nanostructures with highly varied bulk and surface compositions and morphologies must be attainable. And indeed, a number of methods have been demonstrated for creating 1D nanostructures with controllable compositions^{12–17} and morphological variations^{18,19} both coaxial with and lateral to the nanostructure's length, thereby creating nanowire superlattices with electronic and optical properties differing from the analogous bulk material.^{20–24}

In this report we describe a method for precisely controlling the structure along the length of a single nanowire by controlling the instantaneous material flow rate while the nanostructures are in the process of nucleating and growing at constant temperature during the vapor-solid (VS) synthesis of SnO₂ nanowires. The experimental arrangement for nanowire growth in a quartz tube furnace is shown in Figure

1. The carrier gas, Ar (99.998%), is fed into the quartz tube through a solenoid valve that is activated by a computer-controlled power supply, allowing the argon gas flow to be shut off and turned on in a programmable sequence. When on, the steady state flow and pressure inside the tube were, respectively, 100 sccm and 250 Torr. The reagent, SnO powder, was located at the center of the tube where the temperature, set at 900 °C, was most uniform. A large quantity of tin oxide nanowires and nanobelts were found to grow on substrates placed primarily downstream from the source, under these conditions.

Pulsing the argon flow results in pressure changes in the tube, as shown in Figure 2a. When the argon carrier gas is pulsed, nanowires that grow on substrates located a few millimeters upstream from the source were observed to have a controllable, segmented morphology (Figure 2b). The lengths of the segments were found to correlate precisely with the duration of the pulses. For example, with a pulse sequence 7:(3), in which the argon flow was on for 7s and off for 3s, one sees nanowires with thick segments of equal lengths periodically separated by segments of smaller thickness that grow (within tolerable limits) at one of two characteristic angles with respect to the direction of growth of the thicker segments (Figure 3a). With a 35s on, 5s off pulse pattern, 35:(5), the qualitative observation is similar to the 7:(3) situation but with proportionally longer segments (Figure 3b). More complicated nanostructures are shown in Figure 3d–f where the flow-on segments alternate in ratios of 1:2 and 1:2:3 in agreement with the programmed pulse durations. The outcome of many such experiments unquestionably establishes the link between the observed morpho-

* Corresponding author. E-mail: yigalli@yahoo.com.

[†] Department of Chemistry & Biochemistry, University of California, Santa Barbara.

[‡] Department of Materials, University of California, Santa Barbara.

[§] Physics Department, SIUC.

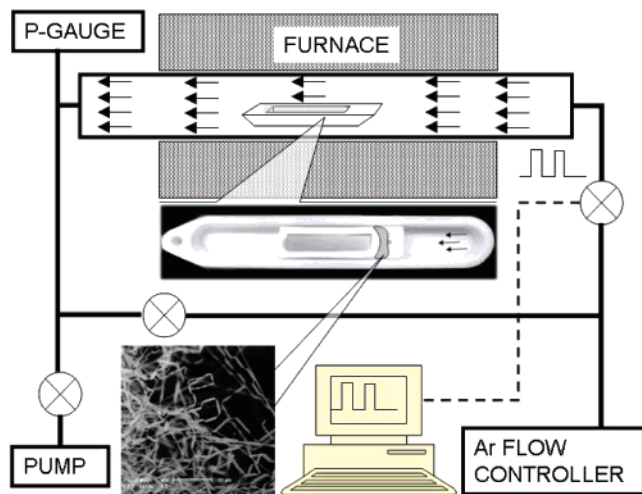


Figure 1. Schematic of the wire growth system.

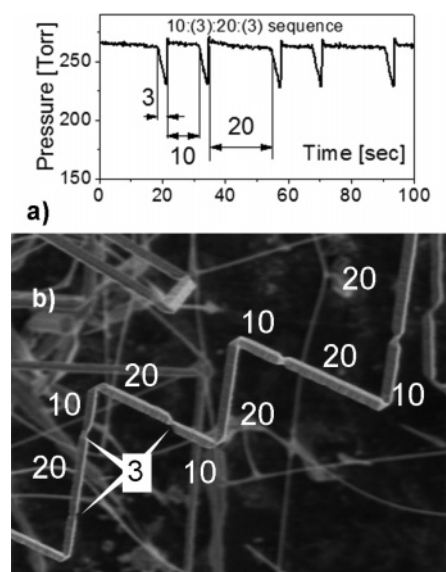


Figure 2. (a) Measured pressure during the 10:(3):20:(3) pulse sequence. (b) SEM picture of the wires grown with this pulse sequence.

logical changes and the programmed pulse structure, which encodes the wire's growth morphology. Hence, these structural changes, which have been observed previously^{11,19} but not correlated with the synthesis conditions, can now be ascribed unequivocally to local pressure and/or flow rate fluctuations. When the carrier gas flow is off, two major morphological changes are observed: (i) the nanostructures continue to grow but with reduced widths; the longer the off period the longer the thin segment (Figure 3a,b,e,f). (ii) the growth direction changes by approximately $\pm 45^\circ$ with respect to the direction of growth of the thicker segment. When the argon flow is resumed, the growth direction changes again by approximately $\pm 45^\circ$ so that, depending on the sign of the second 45° turn, the resulting "junction" between two neighboring thick segments grown during the on periods, form either a right angle overall or restore the growth direction but with a lateral shift. These two options are illustrated in Figure 3. The nanowires appear to have a tendency to preserve planarity during their multiple twists

and turns so that (with equal segment lengths) the overall direction of nanowire growth is a linear combination of integral sums of $+45^\circ$ and -45° turns.

To understand the origin of the observed structural changes, we carried out a number of additional experiments²⁵ with the following results and conclusions: (i) SnO vapor (which is composed of small clusters with a stoichiometry $(\text{SnO})_x$ ²⁶) and trace concentrations of oxygen in the Ar carrier gas are the major reactants in the synthesis of the segmented nanowires. (ii) It is the modulations of the flow rate of the carrier gas in the vicinity of the growing nanostructure rather than the hydrostatic pressure oscillations inside the tube that are responsible for the segment formation. (iii) Segmented wire growth is a result of rapid changes in the local supersaturation ratio of SnO vapor in the vicinity of the wires brought about by the change in Argon flow. Morphological modifications due to rapid changes in the growth conditions was reported previously for nanoring synthesis.²⁷

SEM and HRTEM image analysis of the area between the segments (Figure 4a) provided important clues to the morphological changes occurring as the nanowire transitions from thick to thin segments. In Figure 4a, the body of the thick segments appears to be orthorhombic as was observed previously for SnO₂ nanostructures grown under oxygen-deficient conditions,⁴ although we emphasize that this assignment is preliminary. Notably, the HRTEM images show no structural differences between the narrow and wide segments. Nor is there evidence of dislocations, twinning, or any other discontinuity in the crystal structure in the transition region between the segments. This observation leads us to suggest that the segmental growth proceeds epitaxially and that the thick segments grow at a pyramidal tip. This mode of growth is observed frequently in macroscopic, geologically grown crystals such as amethyst and quartz crystals and in other flow-modulated growth systems.²⁸

Qualitatively, we understand the growth to proceed as follows. When the carrier gas is on, there is sufficient oxygen and SnO for the growth to proceed from the tip of the pyramid downward more or less uniformly, this continues the growth of the nanostructure in the axial direction with little change in width. When the carrier gas is pulsed off, the reactant concentration around the pyramidal tip is asymmetrically reduced so that, for statistical reasons, growth along one of the facets of the pyramid becomes favored. In other words, the reactant concentration during the off cycle is reduced sufficiently that one transitions from kinetic to thermodynamic control of the reaction. If so, then growth on the (110) and $(1\bar{1}0)$ facets minimizes the surface energy of the growing nanostructure more than growth on the other two facets of the pyramidal tip. This would result in epitaxial growth on those facets. This is shown schematically in Figure 4b. (We emphasize that identifying the facets presumes the structure to be orthorhombic. Although several of our TEM studies suggest this structure, the assignment is preliminary.) At first, the wire grows at the "wide" mode, with a constant width and a pyramid-like shape. The flux decrease during the flow pulse will cause epitaxial growth stochastically on either side of the pyramid. The selection of the facet depends

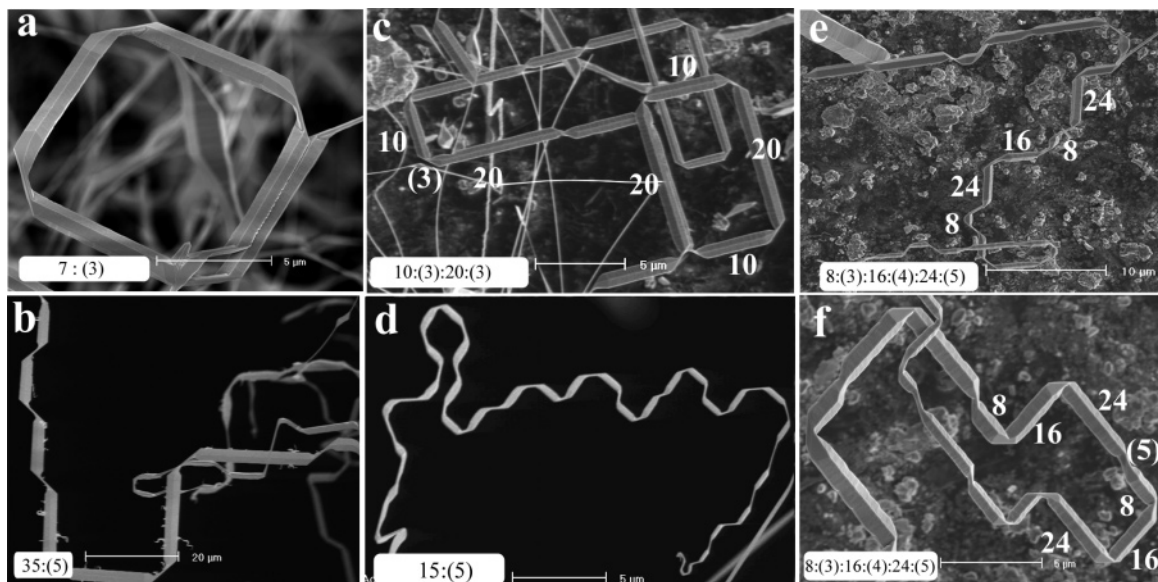


Figure 3. SEM images of the segmented wires grown under various pulsed flow conditions. The images are taken directly off of the alumina crucible. The numbers indicate the duration of the on and off pulses in seconds. The length of the segments is encoded by the pulse duration.

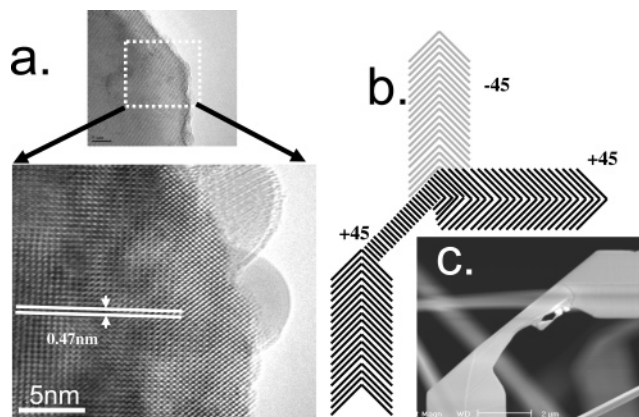


Figure 4. (a) HRTEM picture of a 45° bend. (b) A schematic description of the growth at a pyramidal tip during as the reactant flow changes. (c) SEM image showing a close-up of two consecutive 45° bends. Notice the narrow segment growing out of (and into) one of the pyramid's faces.

on fluctuations of reactant flux. The resulting narrow nanowire begins to grow at 45° with respect to the long axis of the wide segment. After a stable period of narrow growth, the flux resumes to the levels of the wide-growth mode, again, asymmetrically. The pyramidal shape of the tip reappears, and the wire continues to grow as a wide nanowire. Although, obviously this description is highly simplified, it does reproduce the observed nanowire shapes (Figure 4c).

As noted previously,¹⁴ segmentation provides an internal clock for measuring an individual wire's growth rate quantitatively. For example, in Figure 3c the correlation between the 23 s pulse length and the segments in the wires corresponds to a growth rate of ~ 300 nm/s. By using the segmented structure of the nanowire as time markers, one can determine certain characteristics of the kinetics of the nanostructure growth. For example, the segmented wire encoded with a 15:(5) pulse pattern (Figure 5) was found to

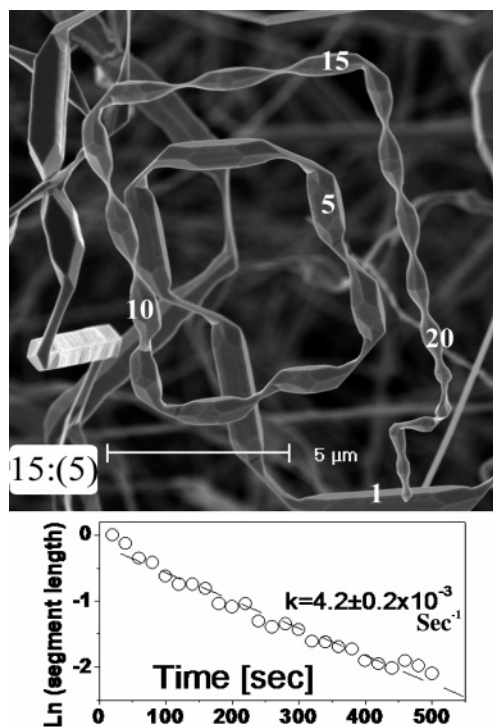


Figure 5. Analysis of the segment lengths of the nanowire shown in the SEM picture. The segments are numbered 1–20 as an aid to the discussion in the text. The segment lengths decrease exponentially in time, purportedly as a result of the oxidation of the SnO reactant in its reservoir.

have segments whose lengths decreased over time. This decrease is most likely due to the fact that the relatively volatile SnO source oxidizes over time to form SnO₂, which seems to be a much poorer reactant. It is sufficient for only the topmost layers of the SnO powder to oxidize in the crucible to impede access to the SnO reactant.

Writing the SnO powder oxidation rate as $dC(\text{SnO})/dt = -k \cdot C(\text{SnO}) \cdot C(\text{O}_2)$, where C denotes the concentration of the

reactants, and assuming the concentration of oxygen to be constant, because it is replenished continuously by the argon gas flow, one derives a pseudo-first-order reaction for the depletion of the SnO reagent: $C(\text{SnO})_t = C(\text{SnO})_0 e^{-kt}$. Because the partial pressure of SnO is proportional to the SnO surface area exposed to the gas phase, it is expected that the growth rate of the wires will follow a first-order decrease, as is indeed observed in a plot of the segment lengths as a function of time (Figure 5).

Apart from its utility as an internal clock, segmented wires can be used in the fabrication of pre-engineered elements of nanodevices. As an example, a nanowire with a nanosized middle section but with micrometer-sized ends could be one way of avoiding contact problems between nanowires and metallic leads.^{29,30}

The results reported here for SnO₂ are not limited to this material but should be observable with other quasi-1D nanostructures synthesized using VS and VLS growth. Combined with pulsed CVD, this can potentially lead to the fabrication of structurally complex nanostructures in which the encoded morphological variations are supplemented by compositional variations.

Acknowledgment. This work was supported by AFOSR DURINT grant F49620-01-0459, by the Institute for Collaborative Biotechnologies through grant DAAD19-03-D-0004 from the U.S. Army Research Office, and made extensive use of the MRL Central Facilities at UCSB supported by the National Science Foundation under award nos. DMR-0080034 and DMR-0216466 for the HRTEM/STEM microscopy. We thank Dr. Tsachi Livneh, Dr. Guosheng Cheng, and Dr. Thomas Tomblor for their assistance.

References

- (1) Cui, Y.; Wei, Q. Q.; Park, H. K.; Lieber, C. M. *Science* **2001**, *293*, 1289.
- (2) Law, M.; Kind, H.; Messer, B.; Kim, F.; Yang, P. *Angew. Chem., Int. Ed.* **2002**, *41*, 2405.
- (3) Pan, Z. W.; Dai, Z. R.; Wang Z. L. *Science* **2001**, *291*, 1947.
- (4) Dai, Z. R.; Gole, J. L.; Stout, J. D.; Wang, Z. L. *J. Phys. Chem. B* **2002**, *106*, 1274.
- (5) Wang, Z. L.; Pan, Z. W. *Adv. Mater.* **2002**, *14*, 1029.
- (6) Arnold, M. S.; Avouris, P.; Pan, Z. W.; Wang, Z. L. *J. Phys. Chem. B* **2003**, *107*, 659.
- (7) Kolmakov, A.; Zhang, Y.; Cheng, G.; Moskovits, M. *Adv. Mater.* **2003**, *15*, 997.
- (8) Comini, E.; Faglia, G.; Sberveglieri, G.; Pan, Z. W.; Wang, Z. L. *Appl. Phys. Lett.* **2002**, *81*, 1869.
- (9) Wang, Y. L.; Jiang, X. C.; Xia, Y. N. *J. Am. Chem. Soc.* **2003**, *125*, 16176.
- (10) Wang, Z. L.; Gao, R. P.; Pan, Z. W.; Dai, Z. R. *Adv. Eng. Mater.* **2001**, *3*, 657.
- (11) Duan, W. J.; Yang, S. G.; Liu, H. W.; Gong, J. F.; Huang, H.; Zhao, X.; Zhang, R.; Du, Y. *J. Am. Chem. Soc.* **2005**, *127*, 6180.
- (12) Gudiksen, M. S.; Lathon, L. J.; Wang, J.; Smith, D. C.; Lieber, C. M. *Nature* **2002**, *415*, 617.
- (13) Lathon, L. J.; Gudiksen, M. S.; Wang, C. L.; Lieber, C. M. *Nature* **2002**, *420*, 57.
- (14) Wu, Y.; Fan, R.; Yang, P. *Nano Lett.* **2002**, *2*, 83.
- (15) Jung, S. W.; Park, W. I.; Yi, G. C.; Kim, M. *Adv. Mater.* **2003**, *15*, 1358.
- (16) Björk, M. T.; Ohlsson, B. J.; Sass, T.; Persson, A. I.; Thelander, C.; Magnusson, M. H.; Deppert, K.; Wallenberg, L. R.; Samuelson, L. *Appl. Phys. Lett.* **2002**, *80*, 1058.
- (17) Cheng, G. S.; Kolmakov, A.; Zhang, Y. X.; Moskovits, M.; Munden, R.; Reed, M. A.; Wang, G. M.; Moses, D.; Zhang, J. *Appl. Phys. Lett.* **2003**, *83*, 1578.
- (18) Wu, Y. Y.; Cheng, G. S.; Katsov, K.; Sides, S. W.; Wang, J. F.; Tang, J.; Fredrickson, G. H.; Moskovits, M.; Stucky, G. D. *Nat. Mater.* **2004**, *3*, 816.
- (19) Givargizov, E. I. *J. Cryst. Growth* **1973**, *20*, 217.
- (20) Björk, M. T.; Ohlsson, B. J.; Sass, T.; Persson, A. I.; Thelander, C.; Magnusson, M. H.; Deppert, K.; Wallenberg, L. R.; Samuelson, L. *Nano Lett.* **2002**, *2*, 87.
- (21) Li, D. Y.; Wu, Y.; Fan, R.; Yang, P.; Majumdar, A. *Appl. Phys. Lett.* **2003**, *83*, 3186.
- (22) Nirmal, M.; Brus, L. *Acc. Chem. Res.* **1999**, *32*, 407.
- (23) Panev, N.; Persson, A. I.; Skold, N.; Samuelson, L. *Appl. Phys. Lett.* **2003**, *83*, 2238.
- (24) Park, W. I.; Yi, G. C.; Kim, M.; Pennycook, S. J. *Adv. Mater.* **2003**, *15*, 526.
- (25) In preparation.
- (26) Zimmermann, E.; Konigs, S.; Neuschütz, D. *Z. Phys. Chem.* **1996**, *193*, 195.
- (27) Hughes, W. L.; Wang, Z. L. *Appl. Phys. Lett.* **2005**, *86*, 043106.
- (28) Oga, R.; Yamamoto, S.; Ohzawa, I.; Fujiwara, Y.; Takeda, Y. *J. Cryst. Growth* **2002**, *237*, 239.
- (29) Wu, Y.; Xiang, J.; Yang, C.; Lu, W.; Lieber, C. M. *Nature* **2004**, *430*, 61.
- (30) Heinze, S.; Tersoff, J.; Martel, R.; Derycke, V.; Appenzeller, J.; Avouris, P. *Phys. Rev. Lett* **2002**, *89*, 106801.

NL051543F